Available online at www.sciencedirect.com
ScienceDirect
Journal of volcanology and geothermal research
Journal of Volcanology and Geothermal Research 160 (2007) 319 – 339
www.elsevier.com/locate/jvolgeores

Origin and stratigraphy of phreatomagmatic deposits at the Pleistocene Sinker Butte Volcano, Western Snake River Plain, Idaho

Brittany D. Brand [a,*], Craig M. White [b,1]

[a] *Department of Geological Sciences, Arizona State University Box 871404, Tempe, AZ, 85287-1404, United States*
[b] *Department of Geosciences, Boise State University, MS1535, Boise, ID 83725-1535, United States*

Received 27 March 2006; received in revised form 7 October 2006; accepted 16 October 2006
Available online 12 December 2006

Abstract

Sinker Butte is the erosional remnant of a very large basaltic tuff cone of middle Pleistocene age located at the southern edge of the western Snake River Plain. Phreatomagmatic tephras are exposed in complete sections up to 100 m thick in the walls of the Snake River Canyon, creating an unusual opportunity to study the deposits produced by this volcano through its entire sequence of explosive eruptions. The main objectives of the study were to determine the overall evolution of the Sinker Butte volcano while focusing particularly on the tephras produced by its phreatomagmatic eruptions. Toward this end, twenty-three detailed stratigraphic sections ranging from 20 to 100 m thick were examined and measured in canyon walls exposing tephras deposited around 180° of the circumference of the volcano.

Three main rock units are recognized in canyon walls at Sinker Butte: a lower sequence composed of numerous thin basaltic lava flows, an intermediate sequence of phreatomagmatic tephras, and a capping sequence of welded basaltic spatter and more lava flows. We subdivide the phreatomagmatic deposits into two main parts, a series of reworked, mostly subaqueously deposited tephras and a more voluminous sequence of overlying subaerial surge and fall deposits. Most of the reworked deposits are gray in color and exhibit features such as channel scour and fill, planar-stratification, high and low angle cross-stratification, trough cross-stratification, and Bouma-turbidite sequences consistent with their being deposited in shallow standing water or in braided streams. The overlying subaerial deposits are commonly brown or orange in color due to palagonitization. They display a wide variety of bedding types and sedimentary structures consistent with deposition by base surges, wet to dry pyroclastic fall events, and water saturated debris flows.

Proximal sections through the subaerial tephras exhibit large regressive cross-strata, planar bedding, and bomb sags suggesting deposition by wet base surges and tephra fallout. Medial and distal deposits consist of a thick sequence of well-bedded tephras; however, the cross-stratified base-surge deposits are thinner and interbedded within the fallout deposits. The average wavelength and amplitude of the cross strata continue to decrease with distance from the vent. These bedded surge and fall deposits grade upward into dominantly fall deposits containing 75–95% juvenile vesiculated clasts and localized layers of welded spatter, indicating a greatly reduced water-melt ratio. Overlying these "dryer" deposits are massive tuff breccias that were probably deposited as water saturated debris flows (lahars). The first appearance of rounded river gravels in these massive tuff breccias indicates downward coring of the diatreme and entrainment of country rock from lower in the stratigraphic section. The "wetter" nature of these deposits suggests a renewed source of external water. The massive deposits grade upward into wet fallout tephras and the phreatomagmatic sequence ends with a dry scoria fall deposit overlain by welded spatter and lava flows.

Field observations and two new ^{40}Ar–^{39}Ar incremental heating dates suggest the succession of lavas and tephra deposits exposed in this part of the Snake River canyon may all have been erupted from a closely related complex of vents at Sinker Butte.

* Corresponding author. Tel.: +1 480 727 6296; fax: +1 480 965 8102.
E-mail addresses: brittany.brand@asu.edu (B.D. Brand), cwhite@boisestate.edu (C.M. White).
[1] Tel.: +1 208 426 3633.

0377-0273/$ - see front matter
doi:10.1016/j.jvolgeores.2006.10.007

We propose that initial eruptions of lava flows built a small shield edifice that dammed or disrupted the flow of the ancestral Snake River. The shift from effusive to explosive eruptions occurred when the surface water or rising ground water gained access to the vent. As the river cut a new channel around the lava dam, water levels dropped and the volcano returned to an effusive style of eruption.

Keywords: phreatomagmatic; Snake River Plain; tuff cone; base surge; lava dam

1. Introduction

Phreatomagmatic eruptions occur when rising magma violently fragments after intersecting and mixing with shallow surface water or groundwater (Sheridan and Wohletz, 1983). In such wet conditions, fragmentation occurs not only by expansion of magmatic volatiles, but principally by energetic interaction between magma and external water (Houghton and Wilson, 1989). The degree of fragmentation, as evidenced by particle size, is a function of melt composition, flux rate, water-melt mass ratio, confining pressure, viscosity difference, and mixing efficiency (Wohletz and McQueen, 1984; Buettner and Zimanowski, 1998; White and Houghton, 2000; Morrissey et al., 2000). The nature of the overall depositional sequence in phreatomagmatic deposits is controlled by a number of variables including the source and amount of external water, the degree to which the volcano is able to seal itself off from external water, and how easily the volcanic edifice is eroded after deposition (Lorenz, 1986; White, 1996).

This paper describes the voluminous sequence of basaltic fragmental deposits produced by phreatomagmatic eruptions of the Pleistocene Sinker Butte volcano (Figs. 1 and 2). Because these deposits are exposed in continuous outcrops in the walls of the ~200-m-deep Snake River Canyon, they afford a rare opportunity to study the complete depositional record from the onset of phreatomagmatic explosions to their conclusion. Moreover, the Sinker Butte tephras can be traced for about 7 km along the canyon walls, so lateral variations can be documented with confidence. The main objectives of the study were to determine the overall evolution of the Sinker Butte volcano while focusing particularly on the tephras produced by its phreatomagmatic eruptions. Our interpretation recognizes three main episodes in the eruptive history of the Sinker Butte volcano: an initial effusive phase that produced numerous thin pahoehoe lava flows, an intermediate Surtseyan-style phreatomagmatic phase that built a large tuff cone on top of the low edifice built by the flows, and a final magmatic phase in which spatter and lavas filled the crater of the tuff cone and flowed as much as 10 km from the vent. We show that the nature of the

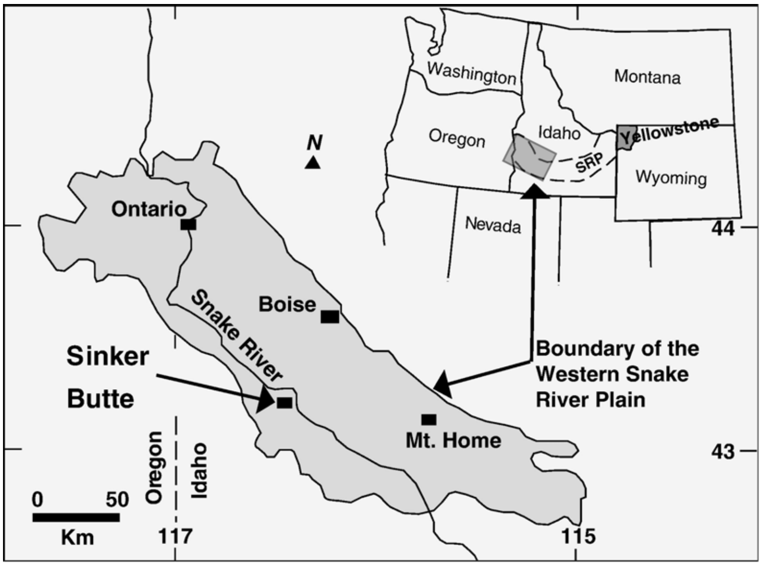

Fig. 1. Site location of Sinker Butte within the boundary of the Western Snake River Plain, Idaho, USA (43° 14 min north latitude and 116° 23 min west longitude).

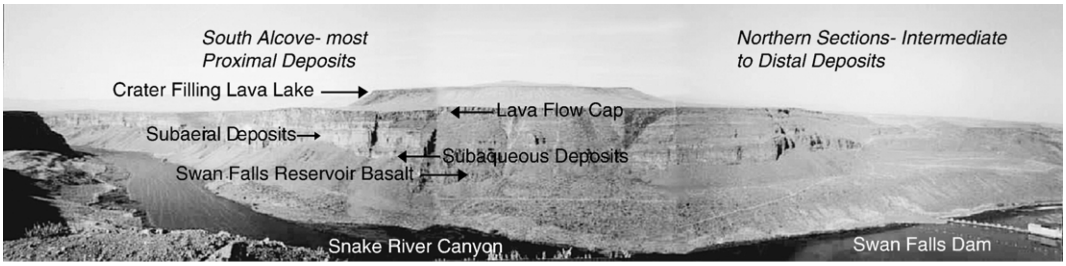

Fig. 2. Photo-mosaic of Sinker Butte looking west. The crater-filling lava lake that forms that highest point of the butte is 1 km across.

fragmental deposits varies substantially both vertically and laterally throughout the sequence, and suggest these deposits indicate rapid changes in vent conditions, depositional mechanisms, and depositional environments.

2. Regional setting

The Snake River Plain (SRP) volcanic province extends from the southwestern corner of Oregon, northeastward across the state of Idaho, to the Yellowstone Plateau in Wyoming (Fig. 1). The SRP volcanic province has been the site of voluminous bimodal volcanism during the last 16 million years, and its origin has been attributed to the passage of North America over the Yellowstone hotspot (e.g. Pierce and Morgan, 1992). In contrast, the western SRP is a northwest trending complex graben that intersects the main SRP-Yellowstone trend near the city of Twin Falls, Idaho. It is 300 km long and about 70 km wide, and contains between 1 and 2 km of basin fill. Subsidence in the western SRP began about 10–11 Ma and was coincident with the shift from silicic to mafic volcanism in southwestern Idaho (Mabey, 1982; Bonnichsen and Godchaux, 2002).

As the western SRP subsided it was occupied by a succession of freshwater lakes, the largest of which is commonly referred to as Lake Idaho (Malde and Powers, 1962). It has been suggested that as the North American continent migrated over the Yellowstone hotspot, the topographic divide shifted and the captured runoff raised the level of Lake Idaho, causing it to reach its spill point (3600 m) around 4 million years ago (Wood and Clemens, 2002). Down-cutting of the outlet progressively lowered lake levels during the next 2–3 million years. It appears likely that the lake had largely disappeared by about 1.6 Ma, because braded stream deposits of this age extend all the way to the outlet area at the northwestern end of the western SRP (Othberg, 1994). Smaller, intermittent lakes probably existed in the western SRP for a long time after Lake Idaho drained. In the area of the western SRP where Sinker Butte is located, Malde (1987) identified evidence for four events in which water of the ancestral Snake River was impounded by lava dams between about 1.7 and 1 Ma.

Sporadic episodes of basaltic volcanism produced a wide variety of hydrovolcanic features in the western SRP during the last 10 million years. Hyaloclastites, pillow deltas, invasive flows, debris flows, tuff cones, tuff rings and maars are all well represented in deposits and landforms associated with the more than 400 volcanoes and eruptive points that have been recognized in this region (Godchaux et al., 1992). The greatest variety of hydrovolcanic features was produced by the flare up of western SRP tholeiitic magmatism that occurred between 2.2 and 0.7 Ma, during and immediately following the draining of Lake Idaho. Earlier basaltic volcanism peaked between 9 and 7 Ma and is associated with hydrovolcanic deposits such as hyaloclastites, pillow breccias and invasive lavas. This episode produced few tephra deposits typically associated with tuff cones and tuff rings, and most of these older units are interpreted as having been erupted beneath the surface of a deep lake (Godchaux and Bonnichsen, 2002).

3. Sinker Butte volcano

Sinker Butte is the largest of the remnant hydrovolcanic structures in the western SRP. The present Snake River Canyon dissects the eastern and southern flanks of the edifice, exposing continuous sections as much as 300 m high for more than 7 km along the canyon walls. Exposures are remarkably clean, owing in part to the catastrophic Bonneville flood, which scoured the canyon walls at about 14 ka (O'Conner, 1993). Godchaux et al. (1992) published the first description of the volcanic deposits at Sinker Butte, noting that the lowest exposures in the walls of the Snake River Canyon contain a sequence of lava flows, which they named the Swan Falls Reservoir basalt. As much as 100 m of phreatomagmatic tephra overlying the lavas, which they interpreted as being the medial and distal facies of a very large Surtseyan tuff cone. Godchaux and co-workers noted that the tephra sequence is capped by lavas and welded spatter, and that Sinker Butte lavas appear to have spilled out of the tuff cone crater and flowed up to 10 km to the south, where the presence of a pillow delta indicates they entered standing water. Based on the published K–Ar ages of Amini et al. (1984), Godchaux et al. (1992) suggested that the tephras are as much as 2 million years younger than the Swan Falls Reservoir basalt. They also proposed that the initial eruptions of the Sinker Butte volcano took place about 100 m beneath the surface of a large lake, and that most of the tephras are subaqueous hyaloclastites that accumulated on top of the older basalts exposed on the lake floor. In their interpretation, the volcano followed an emergent progression from subaqueous eruptions, through late-stage subaerial phreatomagmatic explosions, to a final stage of magmatic (Hawaiian) eruptions.

Two new ^{40}Ar–^{39}Ar dates of samples from lava flows immediately above and below the section of tephras exposed in the canyon wall provide evidence for a revised interpretation for the evolution of the Sinker Butte center (Table 1). The dates were obtained for plagioclase separates at the Noble Gas Spectrometry Laboratory at Oregon State University. Basalt at the base of the Swan Falls Reservoir section, directly below the phreatomagmatic tephras, yielded an incremental-heating, weighted plateau date of 1.25±0.22 Ma, and a plateau date of 1.17±0.18 Ma was obtained for the capping basalt overlying the tephras. The substantial overlap of the two dates indicates that the Swan Falls Reservoir basalts, the phreatomagmatic tephras, and the capping lavas could be approximately coeval. Moreover, the dates suggest that eruptions that formed the Sinker Butte tuff cone post-dated the draining of Lake Idaho by about 0.3 to 0.4 million years. In the discussion below, we address the possibility that the entire section exposed in this part of the canyon was produced by a prolonged series of eruptions from the same center, and that the thick section of tephras was deposited when the volcano temporarily reverted to a phreatomagmatic eruptive style midway through a sequence of effusive eruptions.

Table 1
^{40}Ar–^{39}Ar dates of lava flows from Sinker Butte

Sample No.	Material	Amount	Age	2 s.d.	% ^{39}Ar	Steps (plateau /total)
CM-120[a]	plagioclase	137 mg	1.21 Ma	0.19	100.0	7/7
CM-121[b]	plagioclase	129 mg	1.17 Ma	0.22	100.0	6/6

[a] Swan Falls Reservoir basalt. UTM (NAD27) 478667, 55043; elev. ≈ 750 m.

[b] Sinker Butte basalt. UTM (NAD27) 478685, 55013, elev. ≈ 905 m.

4. Lower effusive lavas

Most of the flows exposed in the canyon walls are 1 to 2 m thick inflated pahoehoe with oxidized ropy flow tops consistent with their having been emplaced on a dry surface. None of the sections we examined showed evidence for any accumulation of lake sediments or development of paleosols between basalt flows. However, near the middle of the section, a few flows show clear evidence for interaction with external water. One contains well-developed pillows at its base and the next few flows above it display alteration features consistent with their having been "water affected" (e.g., Godchaux and Bonnichsen, 2002). The flows in the Swan Falls Reservoir basalt section above this horizon again consist of thin pahoehoe that show no evidence that they were in contact with external water.

The contact between the Swan Falls Reservoir basalt and the overlying Sinker Butte tephras is well exposed in the canyon walls, providing an opportunity to view the paleo-topography of the surface on which the tephras were initially deposited (Fig. 2). Exposures on the scale of 10 s of meters show a hummocky paleo-surface with a relief of 1 or 2 m, consistent with a surface made up of interfingering pahoehoe flows. When the contact is traced for several kilometers along the canyon walls, the paleo-surface can be seen to dip southward, away from present-day Sinker Butte, with a slope angle of about 2°. These relations suggest that the Swan Falls Reservoir basalt may comprise a small shield cone centered at Sinker Butte. Canyon exposures to the north of Sinker Butte are complicated by large scale slump faults, making it difficult to reconstruct the original stratigraphic relations on this side of the presumed center.

5. Phreatomagmatic deposits

The hydrovolcanic tephra beds were mapped north, east, and south of the presumed vent. Twenty-three stratigraphic sections ranging from 20 m to 105 m in thickness were measured and described at proximal, intermediate, and distal locations relative to the presumed vent area (Fig. 3).

Eight stratigraphic facies associations were identified, each containing a variety of lithofacies based on variations in grain size, composition, and sedimentary structures. A lithofacies is defined here as a set of shared deposit characteristics, such as grain size, grain type, sedimentary structures, and local deposit geometry. It is

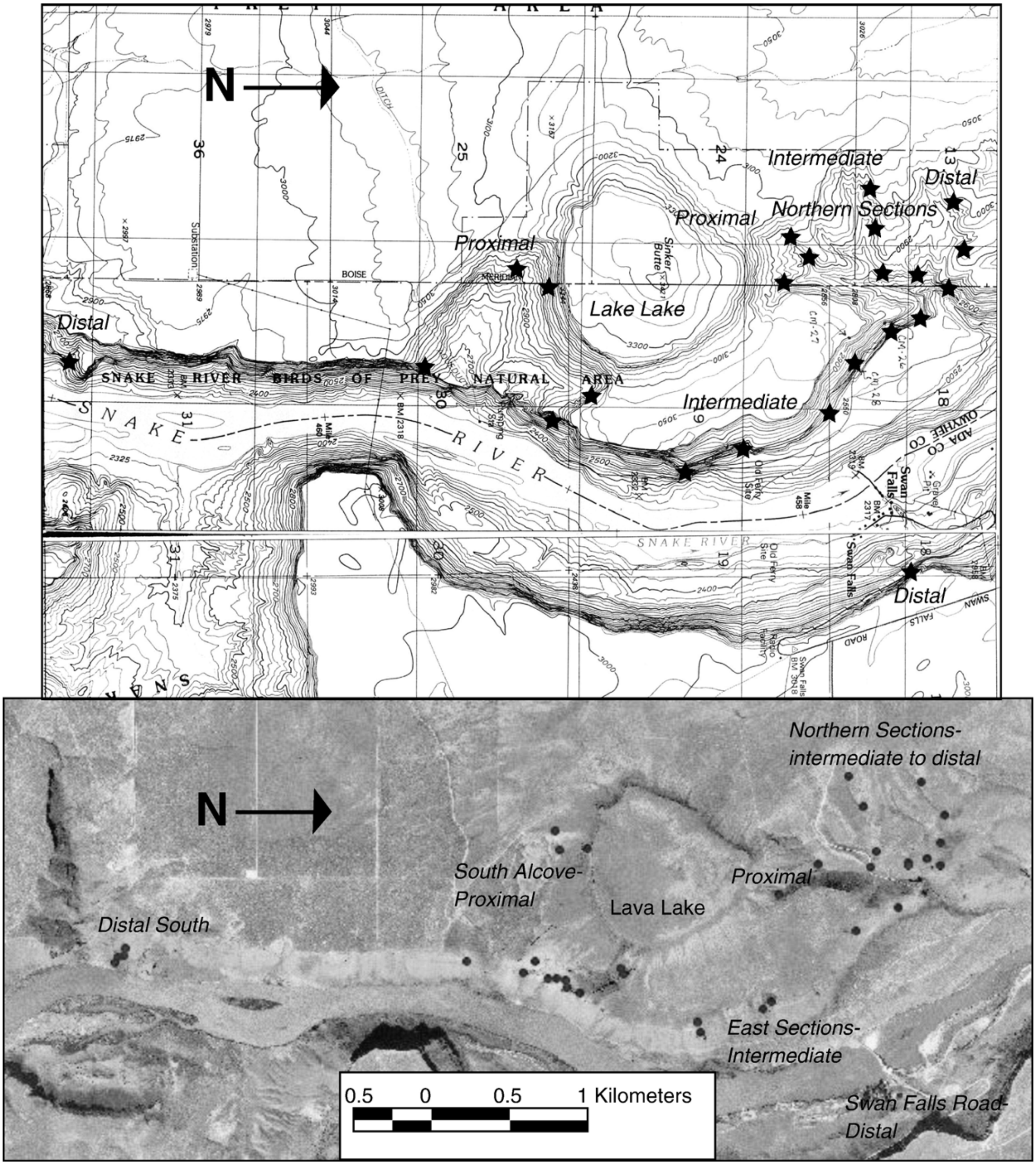

Fig. 3. Topographic map and ortho-photo quad of Sinker Butte. The stars in the topographic map represent the location of each stratigraphic column. The dots in the ortho-photo quad represent areas where GPS measurements were taken during measurements of the stratigraphic columns. The scale in the topographic map is one square mile for each square section.

based on the tephra characterization criteria from Fisher (1961) and Schmid (1981). A facies association (FA) is defined as a mappable subdivision of a stratigraphic section that can be distinguished by the eruptive conditions that produced it. FAs at Sinker Butte are based on vertical facies changes, which reflect variations in vent conditions, mechanisms of deposition, and transportation (e.g. Sohn and Chough, 1989; Németh et al., 2001). FAs may repeat several times throughout the stratigraphy. Table 2 gives a detailed description of

Table 2
Facies association descriptions and interpretations

Facies association	Thickness (m)	Description/interpretation
Major facies association		
1	5–? m thick (highly variable due to paleo-topography and depth of lake)	The beginning of this facies association, where exposed, consistently begins with a meter thick layer of fine, matrix supported, clay to silty clastic sediment and fine-grained volcanic ash with <10% incorporated volcanic grains no larger than fine lapilli. Above this the tuffs incorporate fine-grained accidental particles derived from underlying clastic sediments and juvenile clasts. The Sinker Butte juvenile clasts include fine-ash matrix and phenocrysts of plagioclase, olivine, and opaques. Juvenile clasts larger than coarse ash are distinguishable from the older accidental basalt clasts because of their very irregular, fluidal shapes. Accidental fragments are entrained older basalt, siltstone, and silty to sandy clastic sediments (quartz in composition). The sedimentary structures throughout this unit vary greatly depending on location around the edifice. In some areas the deposits are massive with fining upward sequences; others display repetitive Bouma-sequence sedimentary features; and yet other areas show cross stratification and channel scours. Soft sediment deformation structures were abundant; however, the deposits lacked accretionary lapilli, armored lapilli, palagonite, and the primary depositional features typical of surge and fallout. *Because of such a diversity of sedimentary structures and general lack of primary features typical of surge and fallout deposition, these deposits are interpreted to have been dominated by secondary re-working under subaqueous conditions during the initial platform building stage of the Sinker Butte phreatomagmatic eruption.*
2	3–5 m	Massive and cross-stratified tuffs and lapilli tuffs. FA 2 is generally dark gray in color and consists of massive, clast supported, poorly sorted fine ash to medium blocks. Clasts include accidental fragments (coarse ash to blocks; 40–60%) of older basalt, siltstone, and river gravel, and a higher proportion of juvenile basalt fragments (coarse ash to medium lapilli; 10–20%) in a fine-ash matrix (10–50%). Sedimentary features vary from large channel-type scours to smaller lenticular elongated pockets of coarse lapilli juvenile basalt fragments. In some areas, very low angles cross-strata extend for several meters. In other areas, crude planar-stratification is present evidenced by grain alignment. Steeply dipping cross-strata and trough cross beds can occasionally be found at the top of the unit. Large blocks thought to be ballistics are present in parts of the FA but tend not to have associated underlying bomb sags. No accretionary or armored lapilli were documented, and grading alternates vertically from normal to reverse. *Similar to subaqueous FA 1, these deposits are interpreted to have been dominated by secondary re-working under alternating subaqueous-subaerial conditions due to the rapid rise and fall of water behind the lava dam (discussed in more detail in the text). The lenticular beds and channel scour and fill deposits could have been caused by channelization of a partially or intermittently exposed platform. The massive, poorly sorted deposits were likely formed by erosive subaqueous debris flows caused by steepening of the volcanic platform due to the rapid influx of accidental and juvenile material erupted from the vent. The increase in juvenile material may reflect less water obtaining access to the vent. Multiple types of cross-stratification found close to the subaqueous-subaerial contact are interpreted to be caused by wave action re-working the volcaniclastic sediment just beneath surface of the lake. Similar depositional features are observed at Pahvant Butte, Utah (White, 1996). This FA is an important stratigraphic marker as it occurs just below the subaqueous-subaerial contact.*
3	5–30 m	This FA is composed of planar, fine-grained, well sorted, even thickness, and laterally continuous orange palagonitic tuffs. Individual beds are thin, 1–5 cm, and alternate from fine ash to coarse ash. These tuffs contain a mixture of entrained accidental basalt and siltstone, accretionary lapilli, armored lapilli, and juvenile fragments. The deposits range from 70–95% fine ash matrix, 5–20% accidental clasts (larger than coarse ash), 5–10% accretionary lapilli, and typically <5% juvenile clasts (larger than coarse ash). Occasionally ballistic blocks of older accidental basalt are found underlain by large bomb sag structures. Other soft sediment deformation is also present and not associated with ballistics. Many of the planar beds show reverse grading. Proximal to the vent much of this FA is vesiculated. Thin (<5 cm) interbeds of coarse ash to fine lapilli comprised predominately of juvenile material (70–95% juvenile cinders, <10% accidental clasts, <10% ash matrix) are common. Higher in the section the individual beds become thicker (up to 25 cm), the grains become coarser (alternate from coarse ash to fine lapilli), and the juvenile interbeds become thicker, coarser, and more abundant. *The multiple, thin, even thickness, planar beds are indicative of fallout deposits from a pulsating phreatomagmatic eruption.*
5	>0.5–10 m	This FA is composed of palagonitic cross-stratified lapilli tuffs, massive tuffs, and planar tuffs with reverse grading. The cross-strata are typically low-angle, gently dipping, and show a combination of progressive cross-strata, stationary cross-strata, and antidune cross-strata; however, the

		dominant dune forms are antidunes. These antidunes commonly truncate underlying cross-strata, and show grain accretion predominantly on the stoss side of the bedform. Intermediate to distal from the vent massive and wavy-planar beds with reverse grading are more common along with the cross strata, but antidunes are still dominant. Most distal to the vent the base-surge deposits are characterized by reverse graded planar beds, and fine cross strata displaying pinch and swale structures. The wavelength, amplitude, and dip of the cross-strata decrease linearly away from the vent. Proximal to the vent the strata are large with wavelengths of ~6 m and amplitude of ~1 m; medial to the vent (~1.2 km distance) the average wavelength decreases to ~4.5 m, and the amplitude to ~0.25–0.85 m; and distal to the vent (>1.5 km distance) the average wavelength decreases to <0.5 m, and the amplitude to ~0.01 m. *FA 5 is interpreted to be the result of multiple energetic base surge currents. The antidune structures and presence of accretionary lapilli and vesiculated tephras indicate that the base surges at Sinker Butte were "wet", i.e. they were three-phase flows consisting of gas, particles, and liquid water. Based on MFCI experiments (e.g. Wohletz and McQueen, 1984; Buettner and Zimanowski, 1998), This suggests a water-melt ratio ≥0.5 at the vent.*
6	3–15 m	FA 6 has a gradational transition from FA 3. Higher in the stratigraphic sections, FA 3 becomes coarser grained, thicker, and incorporates a higher percentage of juvenile grains. Interbeds of the thin juvenile rich layers of fine to coarse lapilli present in FA 3 also become thicker, coarser, and occur more frequently. The gradation into FA 6 occurs when the juvenile beds begin to dominate the deposits. The composition is 80–90% fine to coarse juvenile lapilli, <10% accidental lithics, and no accretionary lapilli. The fine-ash matrix varies, but usually makes up 5–10% of the deposit. The amount of palagonitization in this lithofacies varies from little to none. The individual beds are planar and range in thickness from 6 cm to 0.5 m. *The juvenile beds indicate that external water was having less of an affect producing a more Strombolian-style eruption.*
7	3–15 m	FA 7 consists of a variety of thick, massive lapilli tuffs, and tuff breccias commonly found high in the eruptive sequence erosively overlying FA 6. In some areas around the volcanic edifice this FA contains fine to coarse lapilli, while in others areas it consists of coarse-grained tuff breccia with abundant accidental clasts and some juvenile clasts (<5%) within a medium to coarse ash matrix. The features in the massive FA include normal grading, soft sediment deformation, grain sizes from medium lapilli to between 5–20% fine-coarse blocks depending on location. Many of the large blocks within this FA do not have associated sags; rather, they are "floating" in the finer grained matrix. It is important to note that new accidental lithics of pink siltstones and large rounded river gravel appear in this FA. FA 7 has a sharp transition back into FA 3. *These tephras are interpreted to have been deposited by thick, water saturated debris flows. The massive beds suggest a more continuous, less energetic stage in the eruption caused either by an influx of external water or a lowering in magma mass flux. The abundant soft sediment deformation suggests a significant influence of external water, and the new accidental clasts suggest the zone of fragmentation may have been coring deeper into the subsurface.*
8	5–35 m	This FA is found at the highest point in the eruptive sequence indicating the last stage of the eruption. It consists of red scoria deposits capped by basalt lava flows, a late stage lava-lake, and many radiating dikes and sills found intruding throughout the tuff cone walls. *This represents an effusive stage of the eruption where the magma was no longer being affected by, or interacting with, external water.*
Minor and Localized Facies Associations		
4	~40 m exposed	This FA consists of two tuff breccias found high within the southern alcove. One of the tuff breccias dips away from the vent at 20°SE, and one dips into the vent at 15°–33°NW. The inward dipping strata consist of thick, massive, steeply dipping erosive beds that truncate each other and have crude planar stratification evidenced by grain orientation. The grains range from fine ash to coarse blocks with a mean grain size of medium lapilli. The clasts are composed of ~10% juvenile fragments, 40–70% accidental fragments, 10–25% accretionary and armored lapilli, and 20–40% medium ash matrix. Blocks of accidental basalt compose 10% of the FA, and increasing in abundance to ~50% higher in the stratigraphy. The outward dipping strata are predominantly planar bedded and internally massive with occasional crude planar stratification due to clasts alignment. The beds range from 0.5 to 1.5 m thick, and the grains range from medium ash to coarse lapilli and fine blocks (20–30% coarse lapilli, 10–35% fine blocks, 30–40% fine ash matrix). The composition of the grains is ~30% accidental, ~20% juvenile, 30–40% fine ash matrix, and 10–20% accretionary and armored lapilli. The blocks and other large fragments found within this deposit are composed of accidental basalts and comprise 10% of the outcrop, increasing to ~35% higher in the section. The beds have fairly uniform thickness and continue ~40 m before intersecting the late stage crater filling lava lake. *This FA represents the only remnant of the inner and outer cone walls. The beds that dip into the vent and truncate each other at steep angles indicate that some of the built up material avalanched back into the crater. The tuff was deposited mainly by fallout and localized slumping back into and away from the vent.*

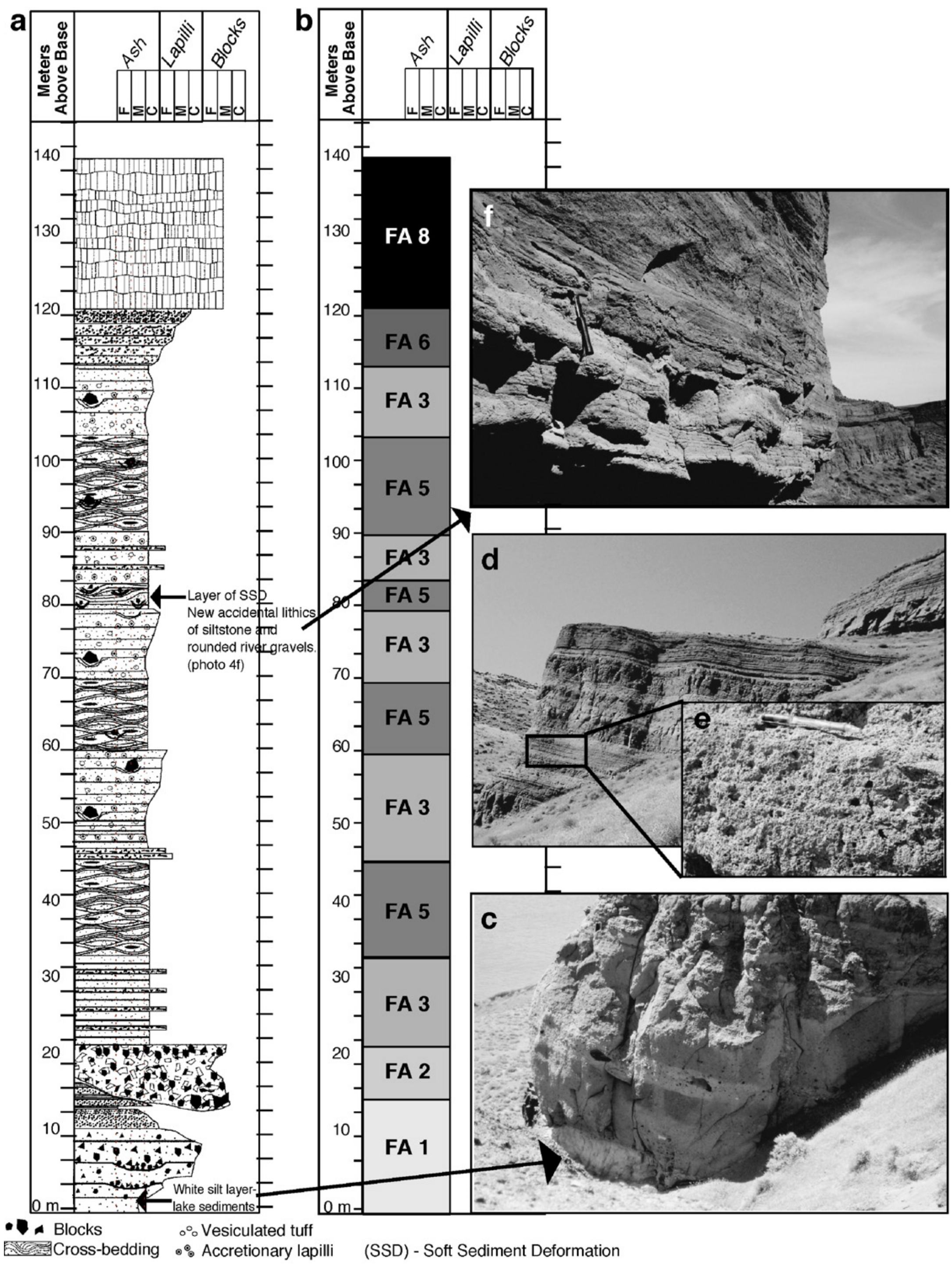

Fig. 4. a) Generalized stratigraphic section from Sinker Butte representing the most proximal deposits exposed (F = fine, M = medium, C = coarse); b) Cartooned section showing locations of FA changes; c) Photograph of the subaqueous deposits (outcrop ∼20 m thick); d) Photograph of the proximal fall deposits dipping at ∼20° away from crater (FA 3; outcrop ∼30 m thick); e) close up of vesiculated tuff within FA 3 (pencil for scale); f) Photograph of a particularly “wet” section (abundant soft sediment deformation) of FA 5 taken from around 80 m above base (hammer for scale).

FAs along with the interpretation for eruptive conditions and depositional mechanism. The types and proportions of grains within each unit are also detailed in this table. Grain percentage was estimated in the field and supported by subsequent petrographic thin section analysis of each FA from multiple locations around the edifice. The Sinker Butte juvenile clasts were distinguished from the older accidental clasts by their fresh appearance, generally greater vesicularity and fluidal shapes.

6. Facies association distribution

Three generalized stratigraphic columns were drafted to represent the presence, thickness, and distribution of the FAs at locations proximal (≤0.5 km), medial (~1.2 km), and distal (≥1.5 km) from the vent (Figs. 4, 6, and 10). Lateral changes in bedding characteristics were determined by constructing fence diagrams. These fence diagrams were created for many places around the volcanic edifice and are based on the data gathered from each detailed stratigraphic section. Where possible, the contacts were traced out for accuracy. One generalized fence diagram was created for this paper and represents the major lateral facies changes from proximal to distal from the vent (Fig. 11).

Fig. 4 represents the vertical FA distribution proximal to the vent. Where exposed, the lowermost pyroclastic deposits just above the Swan Falls Reservoir Basalt consistently begin with a meter thick layer of fine, matrix supported, clay to silty clastic sediment and fine volcanic ash with <10% incorporated volcanic grains no larger than fine lapilli. This lithofacies marks the beginning of FA 1, which in many locations is overlain by FA 2 (Fig. 4a,b,c). As discussed above in Table 2, these FAs are interpreted as having been deposited beneath a shallow lake. The sedimentary structures throughout FA 1 and 2 vary greatly depending on location around the edifice, which is illustrated later when the medial and distal stratigraphic sections are discussed.

The contact between the subaerial and subaqueous deposits, which is invariably sharp around the entire edifice, is represented in Fig. 4 by the contact between FA 2 and 3 at 20 m above base (Fig. 4b). Proximal sections through the subaerial tephras exhibit large regressive cross-strata, planar bedding, and bomb sags. FA 3 in this area is between 5–10 m thick, with

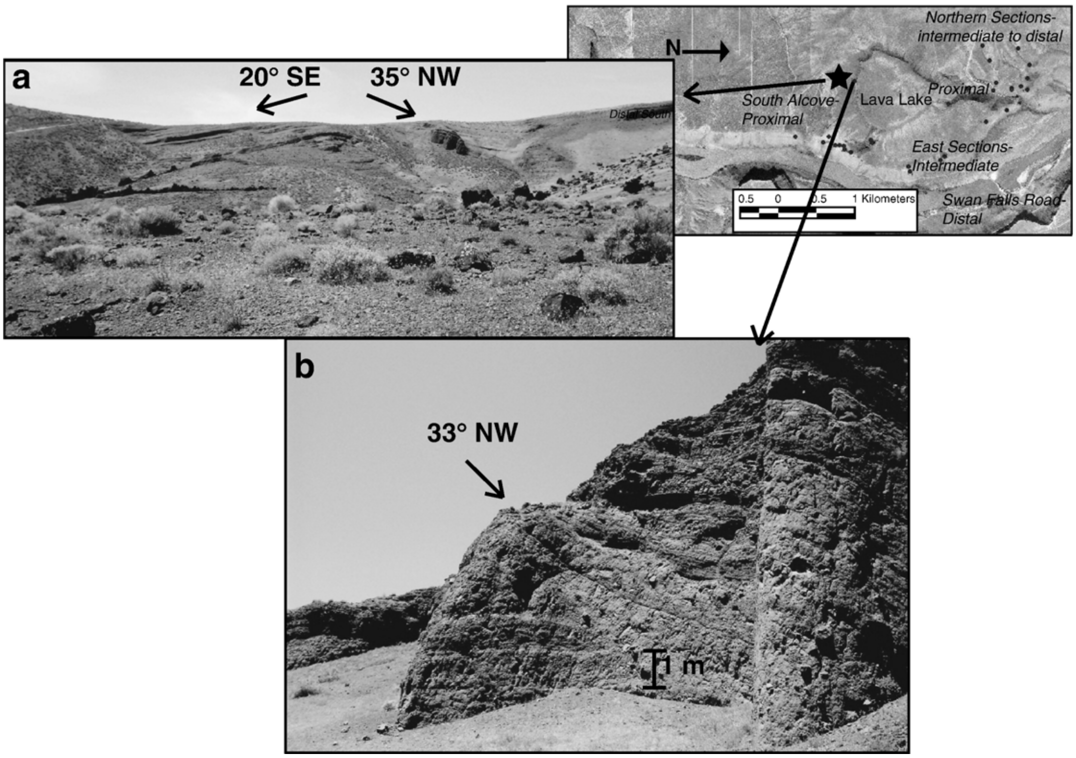

Fig. 5. These pictures represent the crater fill FA 4, a) shows the strata dipping into and away from the vent (photograph ~300 m across); b) shows truncating beds of the inner crater walls.

individual planar, laterally continuous beds between 3 cm and 20 cm thick. The grain size alternates between medium to coarse ash and fine to medium lapilli. The deposits are often vesiculated, show soft sediment deformation beneath ballistics, are highly palagonitized, and contain between 5–20% accretionary lapilli (Fig. 4d,e). Within these 5–10 m thick packages of FA 3, there is a tendency for individual beds to thicken upward (up to 0.4 m thick) and for grains sizes to increase (up to medium-coarse lapilli). In addition, grain types shift to a higher ratio of juvenile material, there are fewer soft sediment deformation features, and accretionary lapilli and vesiculated tuffs are less common. This association probably correlates to FA 6, which is medial to the vent, but differs from it due to the higher percentage of fine ash (~20–30%), and therefore is assigned to FA 3.

FA 5 proximal to the vent is between 2–10 m thick. Individual beds consist of symmetrical and elongated cross strata with an average wavelength of ~6 m, and amplitude of ~1 m (Fig. 4f). The dip, which was measured on both the stoss and lee slide of the cross strata, was at ~20°. The cross strata have a symmetrical and/or anti-dune shape, as accretion most often occurs on the stoss side, with the lee side of the dune elongated. Vertical accretion occurs above the truncation and

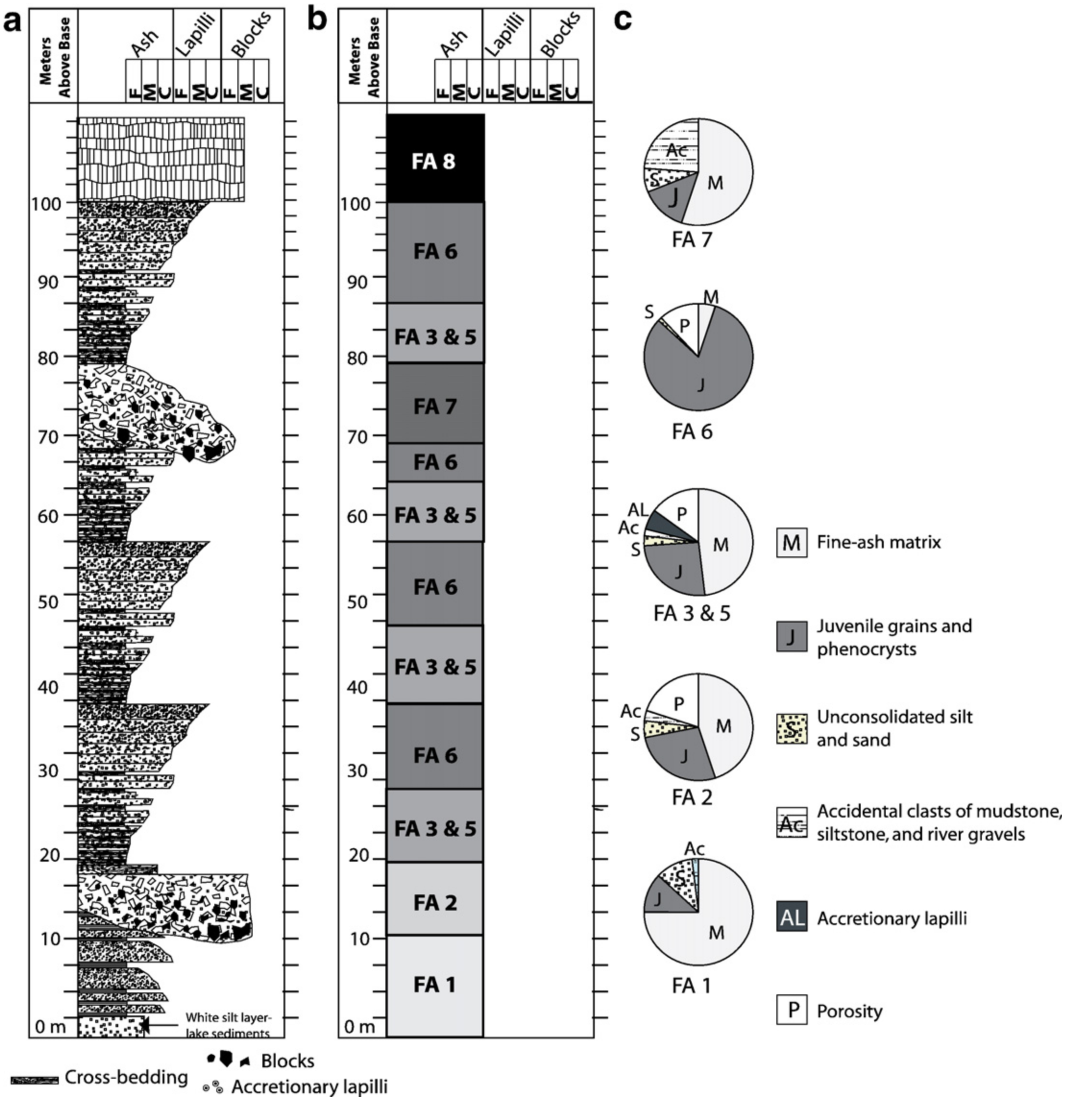

Fig. 6. a) Generalized stratigraphic section from Sinker Butte representing deposits at medial distance from the vent (F = fine, M = medium, C = coarse); b) cartooned section shows locations of FA changes; c) Pie charts represent types and proportions of grains and matrix throughout the FAs and vertical stratigraphy.

beneath the crest. The average grain size of these deposits is fine-medium ash with ~5% armored lapilli and occasionally a few accretionary lapilli. These deposits commonly display a vesiculated texture.

There is evidence for a very wet period around 80 m in the proximal section. These deposits show dominant anti-dune structures with stoss side accretion, a high degree of soft sediment deformation, abundant accretionary lapilli, and new entrained accidental clasts of rounded river gravels and siltstones (the implications of the new accidental lithics is discussed in the next section). Due to the presence of the new accidental material, along with the very wet nature of the deposits and general stratigraphic location, this part of the stratigraphy likely correlates with the same event that deposited FA 7 further from the vent. However, it was not identified as FA 7 because it does not show lahar-debris flow structures.

Towards the end of the section, FA 3 has a gradational contact into FA 6. As discussed in Table 2, FA 6 represents a "drying out" period of the eruption, and is dominated by scoriaceous deposits. This implies a transition into a strombolian-style eruptive phase. Above this lie the effusive deposits of FA 8.

Although it is not shown in the generalized stratigraphic column, the inner and outer crater deposits of FA 4 are present in this area (Fig. 5, Table 2).

The medial and distal sections both begin with the same meter thick deposit of white clastic sediment and fine volcanic ash with <10% incorporated volcanic

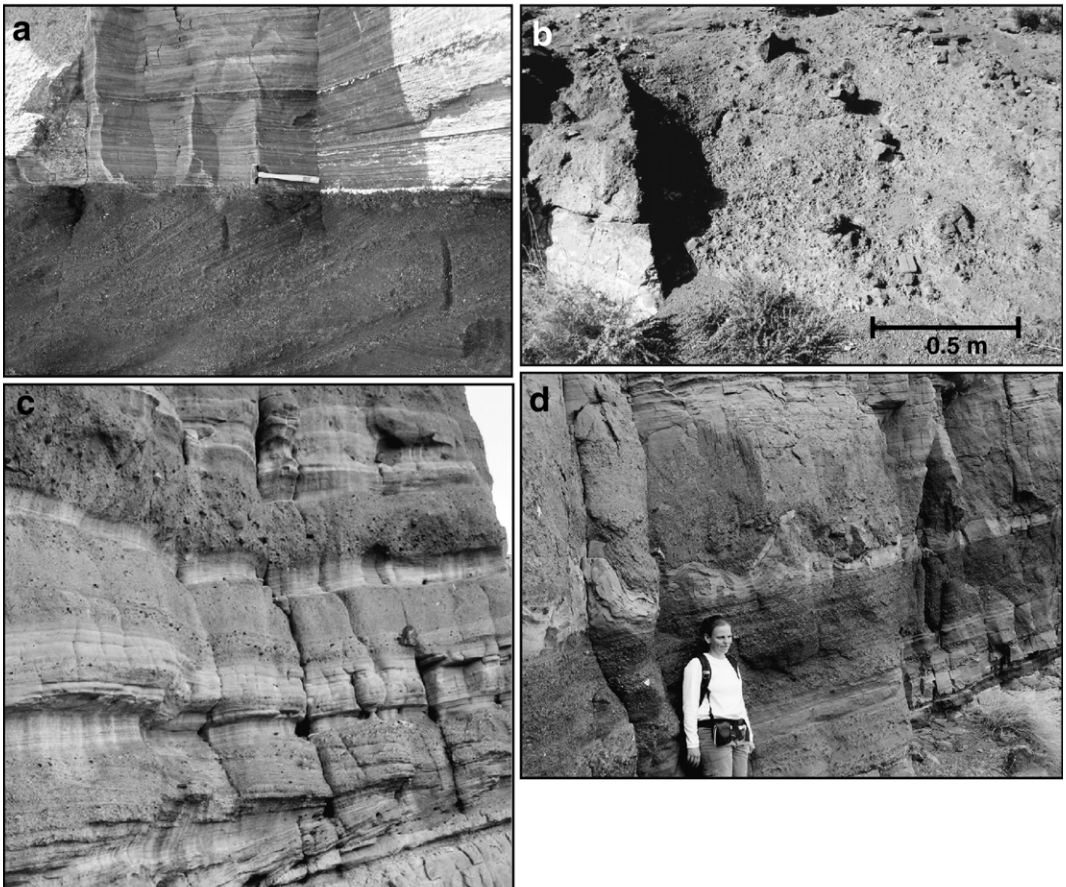

Fig. 7. a) Top of FA 2 displaying cross-bedding consistent with wave-action at the top of the lake; b) Debris flow of FA 2 erosively cutting through FA 1 in medial sections from the vent; c) fining upward sequences within FA 1; d) fining upward sequences and soft sediment deformation features within FA 1.

grains (beginning of FA 1). Overlying this are gray reworked deposits of FA 1 exhibiting Bouma-turbidite sequences, soft sediment deformation, channel scour and fill, and planar-stratification (meters 0–20 in Fig. 6; Fig. 7a). These features are consistent with their being deposited and reworked in shallow standing water. In the medial location, FA 1 is erosively overlain by a thick deposit of FA 2, which is interpreted to represent a debris flow which scoured into the underlying deposits (Fig. 7a). This coarse section of FA 2 ends with high-angle cross-strata and trough cross bedding, just below the contact with the FA 3 and 5 deposits (Figs. 6a and 7b). As discussed in Table 2, and in more details later in the paper, this is thought to have occurred due to the platform growing towards the lake surface and the deposits being reworked and sheared off by the wave-base.

The subaerial deposits medial to distal from the vent consist of a thick sequence of well-bedded tephras with a distinct coarsening and thickening upward trend (meters 20–70 in Fig. 6; Figs. 8, 9, and 10). As the average wavelength and amplitude of the base-surge cross strata decrease with distance from the vent, FA 5 in these areas become thinner and interbedded within the tephra fallout deposits of FA 3. Therefore, medial to distal from the vent, FA 3 and 5 are grouped. Medial to the vent the cross-stratified deposits consist of ~70% medium-coarse grained ash, ~15% fine-grained lapilli, <5% accretionary lapilli, and ~10–12% armored lapilli. They have a wavelength of ~2.5 m, an amplitude of ~0.25 m, and a dip of ~10–12°. When traced laterally the cross strata often transition into planar-wavy deposits (Fig. 8b).

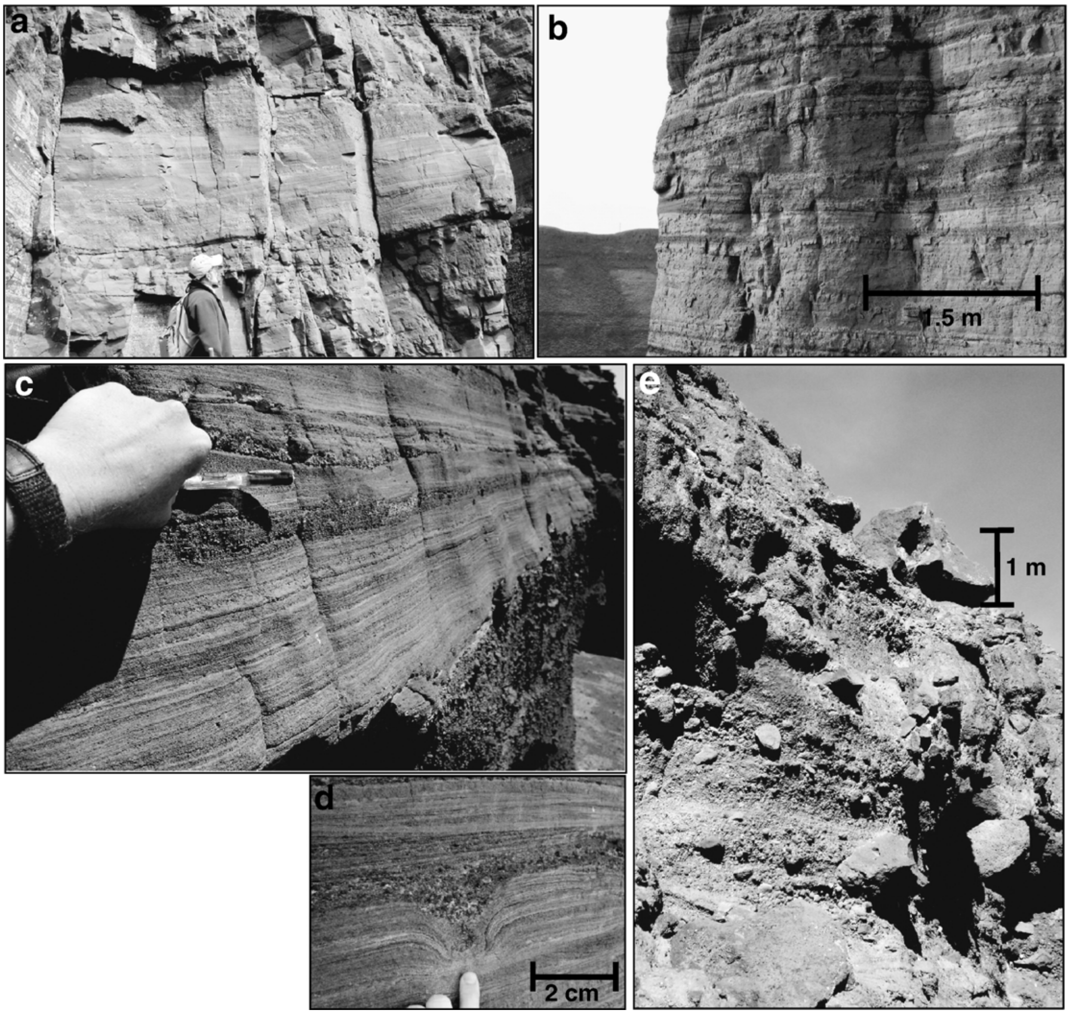

Fig. 8. Subaerial photographs a) Base-surge deposits of FA 5 bounded by the fall deposits of FA 3 (~1 km from vent); b) FAs 3 and 5 ~1.13 km from vent; c) and d) finely laminated fall deposits of FA 3 ~1.4 km from vent exhibiting soft sediment deformation; e) Massive tuff breccia of FA 7, taken ~1.4 km from vent.

The individual planar, laterally continuous fallout deposits of FA 3 are between 3–20 cm thick, and alternate with average grain sizes of fine ash to fine lapilli. These deposits coarsen and thicken up section to 20–50 cm and medium to coarse lapilli, and have a general increase in the percentage of juvenile material larger than coarse ash. This represents the gradation from FA 3 and 5 into the "dryer", Strombolian-style deposits of FA 6, which contains 75–95 percent juvenile vesiculated clasts, and, in localized areas, a 2 m thick layer of welded spatter (above 100 meters in Fig. 6; Fig. 9a,b). This represents a gradual "drying out" during the eruption, and suggests the external water was having less of an effect on the intruding magma resulting in dryer deposits. Pie charts with the average components of each FA with location in the stratigraphic section are included within Fig. 6 to demonstrate this change. The "drying out" sequence represented by the transition from FA 3 and 5 into FA 6 occurs up to three times throughout the stratigraphic sequence (Figs. 6a and 9a).

About 70 m above base, there is an abrupt transition from FA 6 into the massive tuff breccia deposits of FA 7 (Fig. 6). As discussed in Table 2, these were probably deposited as water saturated debris flows, and suggest a renewed source of external water. The pie charts in Fig. 6 illustrate that at this time there is a change in the accidental lithics, as new clasts of rounded river gravels and siltstones are now being incorporated. The appearance of these new clasts indicates downward coring of the diatreme and entrainment of country rock from lower in the stratigraphic section.

The massive deposits grade upward into wet fallout deposits (FAs 3 and 5), and the phreatomagmatic sequence ends with a dry scoria fall deposit (FA 6) overlain by welded spatter and lava flows (FA 8).

The most distal section east of the vent is exposed in a cut along the paved road leading to Swan Falls Dam (Fig. 10). The section has a maximum thickness of 24 m. Overall the succession of deposits here is generally similar to the areas previously described, although the section of tephras is greatly compressed compared to

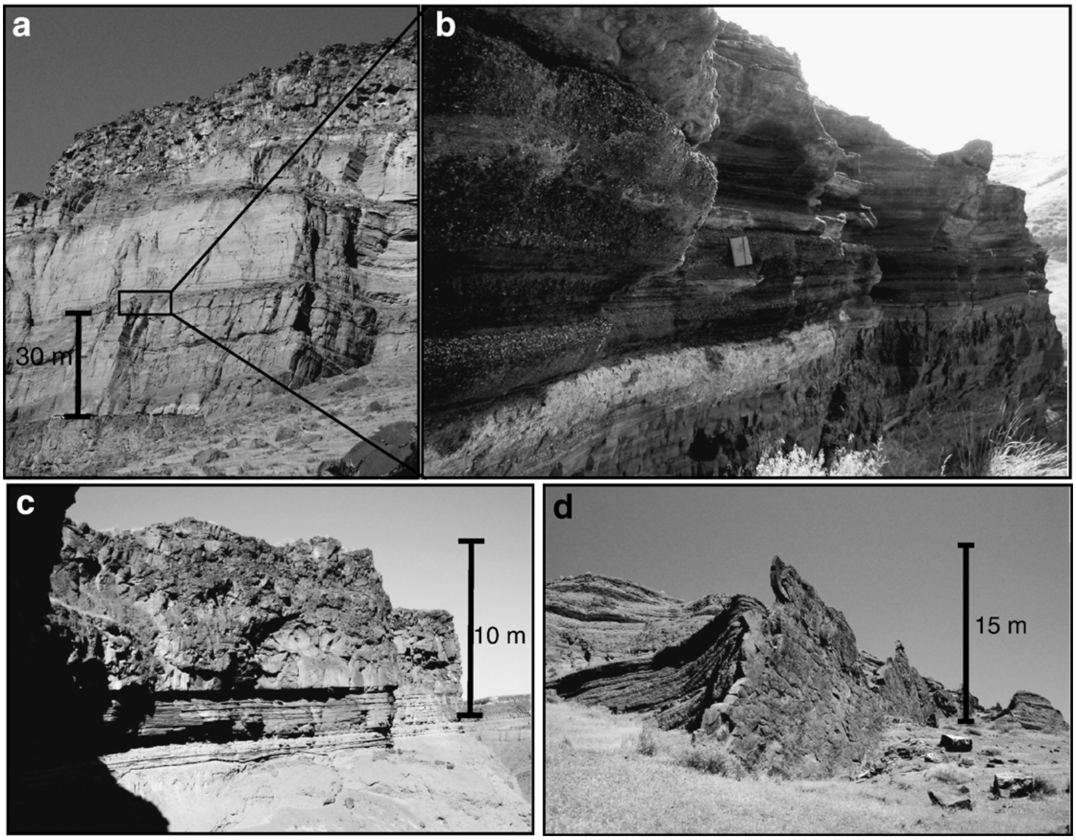

Fig. 9. a) Subaerial photograph of transition from FA 3 into FA 6 (light to dark strata in photograph); b) Close up of the bedded strombolian cinder deposits of FA 6 (notebook-sized field book for scale); c) Transition from FA 6 into the capping lava flow of FA 8; d) One of the many radiating dikes slicing through the subaerial tuff deposits ~0.8 km from vent.

more proximal sections. The lower part of the section consists of white silty sediment, overlain by sub-horizontally bedded tephra containing abundant scoria lapilli (Fig. 10c). This in turn is overlain by 1–2 meters of cross-stratified tephra which contains at least two layers composed of accretionary lapilli (Fig. 10d). The presence of accretionary lapilli is unusual in the basal part of the Sinker Butte tephra section, and they are generally rare or absent in rocks of FA 1. In fact, the tephras in the lowest few meters of this section are more

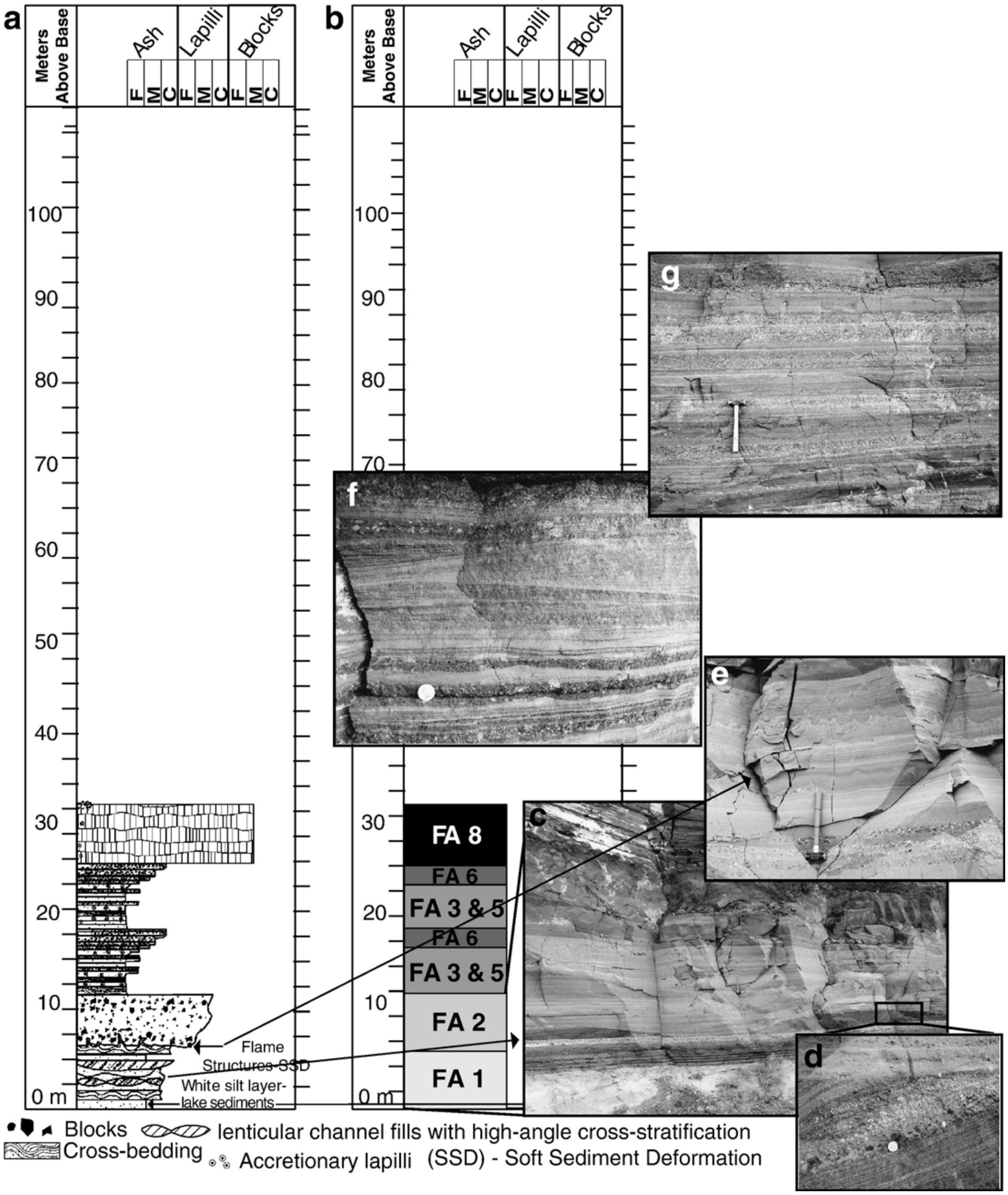

Fig. 10. a) Stratigraphic section from Sinker Butte representing deposits at distal distance from the vent (F = fine, M = medium, C = coarse). This section was measured 2 km from the vent on the east side of the Snake River canyon, east of Swan Falls road where the distal deposits are easily accessible; b) Cartooned section shows locations of FA changes; c, d, and e) Photographs of the lower gray, mostly subaqueous deposits showing planar and lenticular bedding (c; hammer for scale), cross stratification (d; quarter for scale), and soft sediment deformation (e; hammer for scale); f) Finely cross-stratified, fine-grained ash deposits of FA 3 and 5 (quarter for scale); g) Finely planar-stratified, fine-grained ash deposits of FA 3 (hammer for scale).

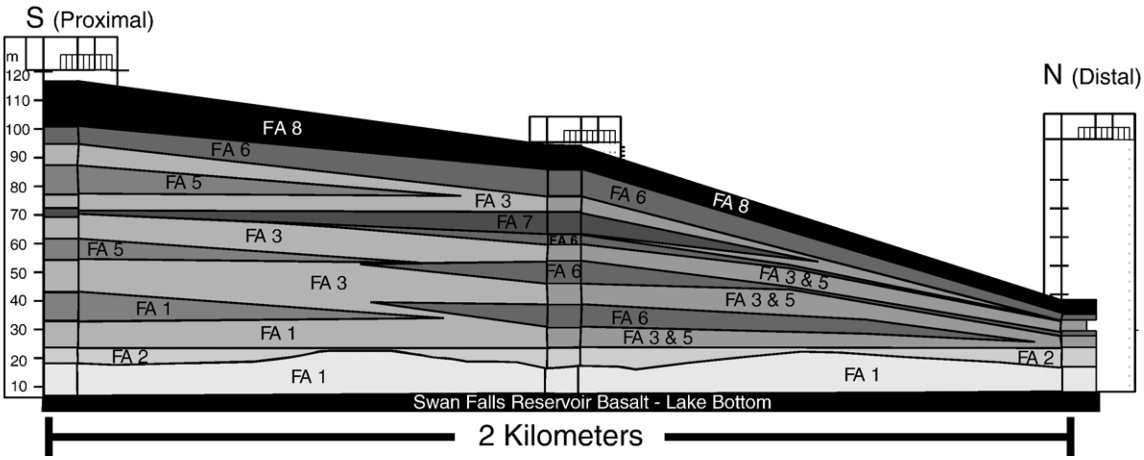

Fig. 11. Generalized fence diagram showing lateral facies changes from proximal to the vent (beginning in the south alcove, Fig. 3) to distal from the vent (2.5 km towards the north).

consistent with deposition in a subaerial environment than a subaqueous one. The next few meters of the section are more typical of FA 1; they consist of thinly laminated, generally fine grained tephras with well developed flame structures and finger-like channels probably associated with dewatering, features consistent with deposition in shallow standing water (Fig. 10e). The upper part of the gray colored, lower half of this section consists of a sequence of thickly bedded, graded deposits with lower contacts that appear to be erosive into the bed beneath.

The typical sharp contact exists between the gray, mostly subaqueous deposits and the orange-brown subaerial deposits of FAs 3 and 5 (Fig. 10). The strata alternate between planar, laterally continuous deposits and cross stratified deposits. The planar strata form 5–20 cm thick beds of extremely well-sorted, fine-medium ash with interbeds of coarse ash. The cross strata consist of fine-medium ash with ~15% accretionary lapilli and <5% armored lapilli. They have a wavelength of ~0.35 m, an amplitude of ~0.01 m, and a dip of ~4° (Fig. 10f). These deposits primarily display pinch and swell structures, are planar to wavy planar, and are difficult to distinguish from the fallout deposits. The deposits then display the cyclic transitions from FA 3 and 5 into FA 6, where FA 6 has a maximum grain size of coarse ash to fine lapilli, and maximum thickness of <1 m. This section ends with a transition from FA 6 into the effusive lava flows of FA 8.

Fig. 11, a generalized fence diagram, illustrates the lateral facies changes with distance from vent.

The subaqueous deposits of FAs 1 and 2 establish the water level at the surface of the lake. Their lower contact reveals the topography at the bottom of the lake, on the upper surface of the Swan Falls Reservoir basalt. The subaqueous sequence, where exposed, always begins

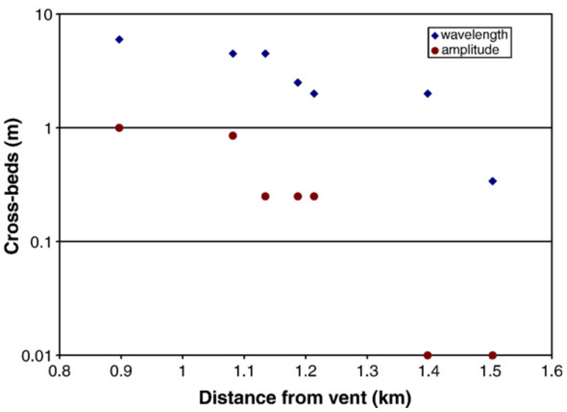

Fig. 12. Wavelength and amplitude (m) versus the distance from the vent (km) on a semi-log plot.

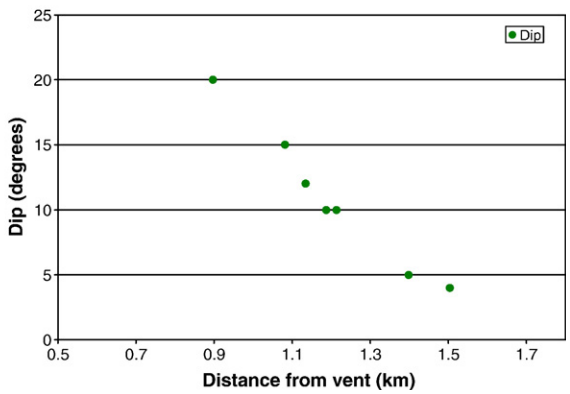

Fig. 13. Foreset dip in degrees versus distance from the vent (km).

with FA 1. FA 2 is not present in all sections; it pinches in and out laterally (Fig. 11). In these sections, the thickness of FA 1 and 2 is around 20 m. However, this varies due to changes in the paleo-topography of the lake bottom. The depth of the lake drastically increases to the south due to an increasing paleoslope, which is evidenced by FAs 1 and 2 found up to 100 m thick 2.8 km south of the volcanic center.

The contact between the subaqueous and subaerial deposits, where exposed, is invariably sharp and abrupt. The fallout-surge FAs 3 and 5 dominate the subaerial stratigraphy around the volcanic edifice. In the proximal and medial fence diagrams it appears as if FA 5 is pinching out. Instead, as previously discussed, it becomes interbedded within the fallout FA 3 and can no longer be distinguished from those deposits. Measurements of the cross strata reveal that the wavelength, amplitude and foreset dip of cross strata decrease approximately linearly away from the vent (Figs. 12, 13, and 14).

Medial from the vent the fallout and surge FA 3 and 5 continue to dominate the stratigraphy, but transition into the Strombolian deposits of FA 6. Where found, FA 6 is locally laterally continuous, but over longer distances has variations in thickness and pinches out.

The massive beds of FA 7 are also found medial to distal from the vent. They tend to pinch out laterally, are thinner towards the vent, and get progressively thicker and coarser further away to a distance of around 1 km (Fig. 11). As discussed previously, there is evidence for a very wet period around 80 m in the proximal section, which likely correlates with the deposits of FA 7 in the medial locations.

The lava flow of FA 8 caps the tephra deposits across most of the area. A lava lake appears to have ponded within the late-stage crater, as evidenced by the 30 inward dip of the uppermost capping lava deposit (Godchaux et al., 1992; Figs. 2 and 3). As bedded pyroclastic deposits are found above the capping lava flow proximal to the vent, it appears the lava flow intruded through the tuff cone walls rather than spilling out of the top. Radial dikes and sills also cut through the tuff cone deposits (Fig. 9) and were likely fed from the central vent of from lava intruding out of the lava

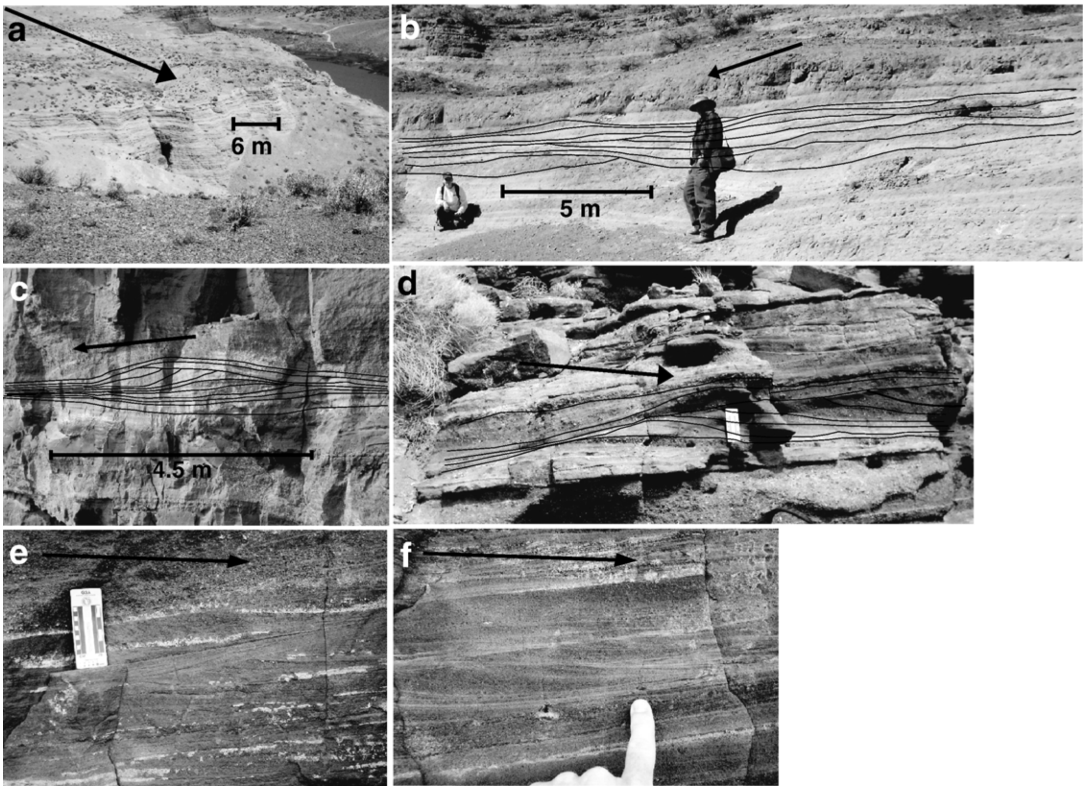

Fig. 14. Photographs of cross strata measured with distance from vent (direction of transport indicated by arrows): a) and b) Distance from vent: 0.8 km, Wavelength: 5–6 m, Amplitude: 1 m, Dip: 20°; c) Distance from vent: 1.13 km, Wavelength: 4.5 m, Amplitude: 0.25 m, Dip: 12–15°; d) Distance from vent: 1.19 km, Wavelength: 2.5 m, Amplitude: 0.25 m, Dip: 10–12°; e) Distance from vent: 1.40 km, Wavelength: 2 m, Amplitude: 0.01 m, Dip: 5°; f) Distance from vent: 1.50 km, Wavelength: 0.35 m, Amplitude: 0.01 m, Dip: 4°.

ponded in the crater. Overall the thickness of the deposits and the grain size decreases distally from the vent.

7. Discussion of the eruptive history interpreted from deposits

7.1. Initial effusive eruptions

The newly acquired radiometric ages for basalts exposed in the Snake River canyon support the interpretation that the Swan Falls Reservoir basalts were produced by the initial eruptions of the Sinker Butte volcano. This differs from the interpretation of Godchaux et al. (1992), who suggested that these lavas were much older than the Sinker Butte deposits. The initial effusive eruptions probably produced scores, if not hundreds, of thin pahoehoe flows. Individual sections in the canyon walls contain as many as 20 flows in succession. We suggest that these lavas may have dammed the ancestral Snake River resulting in the temporary creation of a small freshwater lake. A rapid rise in the water level behind such a lava dam could explain the presence of a few water affected lava flows near the middle of the basalt section. The southward dip of the upper surface of the Swan Falls Reservoir basalts and the presence of a thickening wedge of subaqueous tephras away from the presumed vent area (Fig. 15) are consistent with the presence of a lava-dammed reservoir. If this hypothesis is correct, then tephra deposits on the downstream (northern) side of the proposed lava dam should reflect a different depositional environment; however, as noted above, poor exposures in the canyon north of Sinker Butte, and the lack of any exposures away from the canyon walls, have prevented us from determining the stratigraphy on all sides of the volcano.

7.2. Shift to phreatomagmatic eruptions

The shift from effusive eruptions to a prolonged episode of phreatomagmatic explosions at Sinker Butte can be explained by a process in which water impounded behind a newly formed lava dam rose to a level where it gained access to the vent or came in contact with shallow feeder dikes. Alternatively, a small shift in the location of the vent could have caused magma to begin erupting directly beneath the newly formed reservoir. The change to explosive eruptions appears to have been abrupt, although the contact in one area contains several alternating layers of tephra and lava indicating a brief transition period in which both types of eruptions were taking place. Regardless of whether the vent was above or below standing water when the phreatomagmatic eruptions began, it is reasonable to assume that some of the tephra produced by these explosions would have been deposited in the lake upstream from the lava dam. As the eruption progressed, the ejected material appears to have built a shallow platform of tephra within the reservoir, as evidenced by the subaqueous deposits, FAs 1 and 2. This was observed at hydrovolcanoes such as Surtsey, Iceland (1965 eruption, Kokelaar, 1983) Capelinhos, Azores (1957–1958 eruption; Waters and Fisher, 1971) and Karymskoye Lake, Russia (1996 eruption; Belousov and Belousova, 2001). It is important to note, however, that not all of the deposits overlying basalts at the base of the tephra section are unambiguously subaqueous. As noted above, the lowest few meters of the distal section east of Sinker Butte contain cross-stratified accretionary lapilli tuffs, which are typically more consistent with subaerial base surge deposits.

The lower part of the pyroclastic section contains several fining-upward sequences where the finest material is thinly laminated. This provides evidence for a pulsating eruption rather than a steady vent flux. Debris flows were also emplaced, likely due to instability of the over-steepened, water saturated tephra deposits. Also present in many areas of FA 1 are soft-sediment deformation structures, which indicate rapid influxes of material into the lake (Figs. 4c, 7, and 10e). Water saturated volcaniclastic sediment would be deformed by the weight of the new material, especially if there were density or strength contrasts between adjacent layers. The volcanic-sedimentary platform continued to grow towards the surface of the lake as the eruption progressed. Channel scour and fills can be seen only a meter or so below the presumed subaqueous-subaerial contact, indicating parts of the platform began to channelize as they grew closer to the surface. Tephra building around the vent could have trapped water within the crater of the tuff cone, and partial cone collapses could have released the water quickly causing erosive channels. Channels could also have been formed by water running across an intermittently exposed subaerial platform.

FA 2 is the uppermost FA observed before the subaqueous–subaerial contact. It is only present in some areas of the volcanic-sedimentary platform and tends to pinch out laterally. This FA contains a slightly higher percentage of juvenile material and commonly has an erosive contact where it overlies FA 1. Wave-induced cross-stratification suggests that this FA was very close to the surface of the lake, and the asymmetrical, symmetrical, and trough cross-strata provide evidence

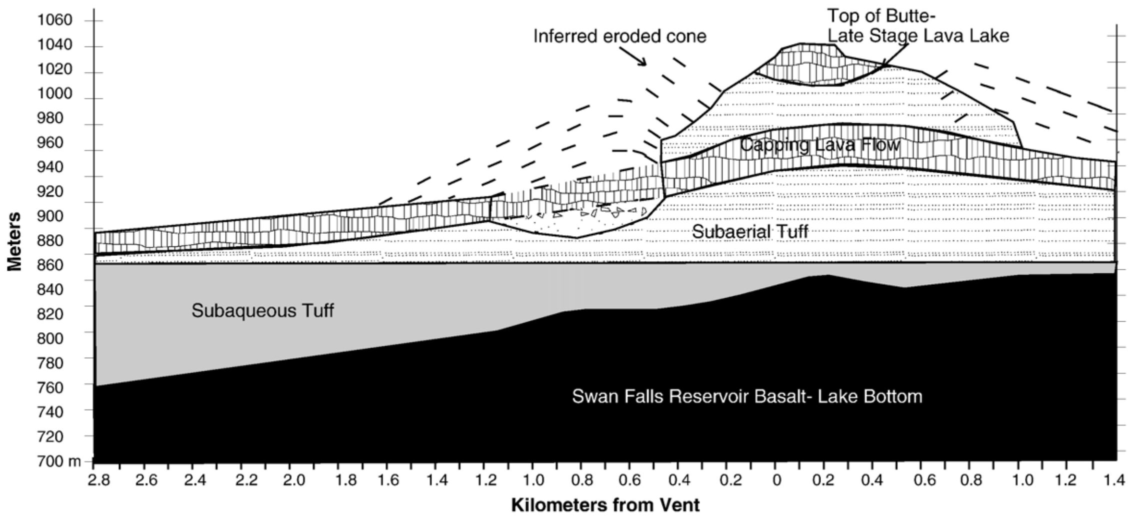

Fig. 15. This is a cross section of the remnant volcanic edifice of Sinker Butte. It illustrates the reconstructed height and width of the eroded cone, the bottom of the lake (between Swan Falls Reservoir Basalts and subaqueous sediments), the deepening lake to the south, and the thickening of subaqueous of deposits away from the vent. The left side of the figure is due south, and the right due north. The crater walls, which are now eroded away, are inferred from strike and dip measurements taken around the edifice. The lava flow appears to have intruded through parts of the unconsolidated tuff cone rather than spilling out from the top, as there are pyroclastic deposits exposed above it in the butte.

for both uni-directional and bi-directional flow. Explosions from the vent could have created currents and waves within the lake creating both uni-directional and bi-directional movement, which would result in these deposit characteristics.

Fragments of disrupted country rock are common in many of the Sinker Butte tephras and include older basalts and sedimentary rocks as well as unconsolidated grains of clay, silt, and sand. Unfortunately, the lithic fragments can not be uniquely correlated with known units in the subsurface because the stratigraphy beneath Sinker Butte is so poorly constrained. The late Miocene and Pliocene basin filling deposits of the western Snake River Plain are a heterogeneous mix of fluvial gravels, deltaic sands and silts, lacustrine mudstones, and intercalated basaltic lavas and tephras. The abrupt facies changes within this sequence make detailed correlations of stratigraphic units nearly impossible.

7.3. Main phase of phreatomagmatic activity

The sharp contact and abrupt change in deposit characteristics observed at the top of FA2 suggests this horizon may mark a brief period of quiescence during which the level of the reservoir dropped and tephras were redistributed by braided streams. The overlying deposits are interpreted to be subaerial because of several characteristics: (a) they contain no evidence of secondary reworking by water, (b) they contain bedforms characteristic of pyroclastic surges, and (c) they are strongly palagonitized, whereas the beds immediately beneath them contain unaltered glass. Although palagonite is typically associated with secondary hydrothermal processes, in phreatomagmatic deposits it can form either simultaneously with deposition or very shortly thereafter if significant amounts of heat and steam are present in the eruption and during deposition (Farrand and Singer, 1992). Because the palagonitic alteration does not cross stratigraphic units and its first appearance is exactly coincident with the boundary of the facies associations, it is unlikely that it formed as the result of a later hydrothermal alteration event.

The changes in grain size and bedding structures observed at the contact indicate a substantial change in the eruption style as well as in the depositional environment. The massive subaqueous FAs contain clasts from medium ash to blocks, whereas the overlying subaerial tephras are composed of fine to medium ash deposited in planar and finely cross-stratified beds. The change here would likely reflect a change in either the amount of water or the magma mass flux, which together control how efficiently the two fluids will mix (e.g. Wohletz and McQueen, 1984; Buettner and Zimanowski, 1998). Petrographic examination of glass shards in tephras from both sides of the contact show they contain the same phenocrysts in roughly the same proportions, therefore the magma temperature and viscosity can be assumed to have been similar. The most likely cause of the shift in eruptive style is a lowering of water level in the reservoir behind the lava dam or a realignment of the river, which reduced the amount of water that gained access to the vent or sub-volcanic plumbing system.

Proximal to the vent, the subaerial deposits are primarily made up of FAs 3 and 5. The extremely fine-grained tephra in the subaerial deposits suggest efficient fragmentation of the magma. However, the presence of accretionary and armored lapilli in both the fall and surge deposits, in addition to the dominant stoss-side accretion of dunes, suggests a moderate amount of liquid water in the surges and/or eruption clouds from which they formed (e.g. Fisher and Schmincke, 1984; Heiken and Wohletz, 1986; Wohletz, 1986). Furthermore, the vesiculated tephras present in the proximal deposits suggest that water contents were high in the jets depositing tephra on the crater rim (Rosi, 1992). This implies that the water-melt mass ratio was high enough that all of the external water could not be flashed to steam. Fuel-coolant interaction studies show similar conditions when the water-melt ratio is equal to or slightly higher than 0.5 (e.g. Wohletz and McQueen, 1984; Buettner and Zimanowski, 1998).

FA 3 dominates the subaerial deposits medial to distal from the vent. However, in the medial to distal regions, these planar beds contain abundant interbeds of FA 5. This is due to simultaneous emplacement of fallout and base surges. As a surge moves laterally away from the vent, it loses heat, solids, and momentum resulting in a decreasing wavelength and amplitude of the cross-stratified base-surge deposits with distance from the vent (e.g. Waters and Fisher, 1971; Wohletz and Sheridan, 1979; Sohn and Chough, 1989; Figs. 12, 13, and 14). The loss of heat results in condensation of steam, which explains the increase in "wet" features such as armored and accretionary lapilli, dominant stoss-side accretion of the dunes, and abundant soft sediment deformation with distance from vent. This may also result in grain size change of the surge deposits with distance from vent. The most proximal deposits contain fine to medium-grained ash, the intermediate deposits contain medium to coarse-grained ash with some fine-grained lapilli, and distal the grain size is again a fine ash. With increasing liquid water due to condensing gases, adhesion of ash would increase, which is evidenced by the increase in armored and accretionary lapilli with distance from source. This would increase the sedimentation rate as the greater effective grain size may exceed the competency of the surge (e.g. Sohn and Chough, 1989).

The deposits within FA 3, including the juvenile-rich interbeds, get coarser-grained and thicker up section. Eventually, the juvenile interbeds within FA 3 begin to dominate and grade into FA 6. This is a repeating cycle that occurs at least three times throughout the eruptive sequence, and it suggests that as the eruption progressed, the influence of external water gradually decreased via either depletion of the external water, increase in magma flux, or a combination of the two. When a higher water-melt mass ratio was again produced, the cycle would start over again. As the amount of external water fluctuated, the eruption alternated between a wet Surtseyan and a dry Strombolian eruption. Coarsening upwards sequences indicate decreasing fragmentation energy, although the multiple planar beds still suggest pulsating explosions (Waters and Fisher, 1971; Fisher and Schmincke, 1984; Heiken and Wohletz, 1986).

There is evidence, in both proximal and distal areas, for a much wetter intermediate stage of the subaerial eruption. This is indicated by massive FA 7, which can be found medial to distal from the vent. While the surge-fallout deposits are results of a water-affected pulsating eruption, the massive beds seem to indicate a more continuous eruption, and the soft sediment deformation associated with most of the massive deposits suggest an increased influence of external water. According to the Wohletz and McQueen (1984) study of explosive FCI experiments, the massive nature of the deposits, along with the larger clasts and blocks, indicate a less energetic stage consistent with a much higher water-melt ratio. The efficiency of fragmentation at this much higher water-melt mass ratio is lower than the ratio that forms the finer-grained planar beds below.

The renewed external water could have come from one of two sources. The first possibility is a small sector collapse in the cone allowing a temporary ingress of lake water to the vent, such as was observed at Surtsey, Iceland (Moore, 1985). However, no such collapse structure was found around the volcanic edifice. The second and more likely possibility is downward movement of the fragmentation zone. New accidental clasts (river gravels and pink siltstone) indicate that as the volcano continued to erupt, the vent cored deeper into the underlying stratigraphy. At this depth the vent may have intersected an aquifer, yielding the excess water that caused the abundant wet eruptive depositional features described above. The introduction of new accidental material supports this interpretation rather than the former.

After this very wet stage, the deposits grade back into the planar FA 3, and again into FA 6. This suggests that once again the eruption was "drying out". The eruption then transitioned into the final effusive stage where external water was no longer gaining access to the intruding magma, resulting in the spatter, lava flows, and dikes of FA 8.

8. Final magmatic phase of eruption

The final FA at Sinker Butte, FA 8, begins with a layer of scoria one to four meters thick followed by a thick lava flow. This represents the point in the eruption where the volcano had effectively become sealed off from external water. The very latest stage of the eruption appears to have created a lava lake within the crater. The lower contacts of this ponded lava dip at ~30° inward to the center of the filled crater. Godchaux et al. (1992) noted that lavas erupted during this phase flowed as much as 7 km south of the crater, where they appear to have entered standing water as evidenced by the presence of a pillow delta. At least 10 radial dikes stand in positive relief where they cut the tephra deposits exposed in the eastern and southern walls of the canyon (Fig. 9d). Several of these dikes appear to merge upward into the lava flows that cap the tephras exposed in the canyon walls, suggesting they may have broken out on the lower slopes of the tuff cone and produced lava flows at secondary vents away from the main crater. There is no direct evidence that indicates the tephra eruptions at Sinker Butte took place from more than one vent, but neither can this possibility be ruled out. However, the main vent area was almost certainly located beneath the lava cap at the top of present day Sinker Butte. This is also the location at which the radial dikes converge and from which they most likely originated.

9. Post-eruptive events

At the time the eruption ceased the volcano had built a broad, probably asymmetrical lava shield overlain by a large tuff cone, which in turn was capped and partially draped by lavas and welded spatter. The entire edifice would have been at least 330 m high and the crater of the tuff cone may have been as much as 1500 m in diameter (Fig. 15). Post-depositional erosion has shaped the butte as it is seen today. The fact that there is little evidence for prolonged erosion by standing water, as has been noted for emergent tuff cones such as Pahvant Butte (White, 2001) and Fort Rock (Heiken, 1971), suggests that the river probably finished cutting a new channel around the lava dam soon after the Sinker Butte eruptions had ceased. It is impossible to tell if the late stage lavas caused any disruption of the upper part of the tephra cone because it has been removed by subsequent erosion (dashed lines in Fig. 15). Later shifts in the channel of the Snake River resulted in the present-day location the Snake River Canyon, which cuts directly through the eastern side of the volcanic edifice where much of the deposits are presently exposed. At approximately 14 Ka the Bonneville flood scoured the canyon walls and may have further altered the exposures of the Sinker Butte tephras (O'Conner, 1993). As it is seen today, the nearly flat, mesa-like summit of Sinker Butte is the erosional remnant of the solidified late stage crater filling lava lake. The elongate platform or shelf that forms the canyon rim below the top of Sinker Butte is a remnant of the late stage lava flows, some of which may have been fed by radial dikes that breached the walls of the tuff cone. The steep sided walls of the canyon below this platform expose the subaerial and subaqueous phreatomagmatic tephras and the underlying Swan Falls Reservoir basalts that formed the initial shield edifice.

Acknowledgments

The authors thank Martha Godchaux, Bill Bonnichsen, and Spencer Wood for many helpful discussions related to our research at Sinker Butte. Comments and suggestions by Amanda Clarke and formal reviews from Pierre-Simon Ross and Sharon Allen were much appreciated as they significantly improved the manuscript. Funding for this research was provided by grants from the Geological Society of America and the Idaho NASA Space Grant Consortium to B.D.B., and by a grant from the Petroleum Research Fund (ACS-PRF#36899-B) to C.M.W.

References

Amini, M.H., Mehnert, H.H., Obradovich, J.D., 1984. K–Ar ages of late Cenozoic basalts from the Western Snake River Plain, Idaho. Isochron-West 41, 7–11.

Belousov, A., Belousova, M., 2001. Eruptive process, effects and deposits of the 1996 and the ancient basaltic phreatomagmatic eruptions in Karymskoye Lake, Kamchatka, Russia. Special Publication of the International Association of Sedimentology 30, 35–60.

Bonnichsen, B., Godchaux, M.M., 2002. Late Miocene, Pliocene, and Pleistocene geology of southwestern Idaho with emphasis on basalts in the Bruneau-Jarbridge, Twin Falls, and Western Snake River Plain regions. In: Bonnichsen, B., White, C.M., McCurry, M. (Eds.), Tectonic and Magmatic Evolution of the Snake River Plain Volcanic Province. Idaho Geological Survey Bulletin, vol. 30, pp. 233–312.

Buettner, R., Zimanowski, B., 1998. Physics of thermohydraulic explosions. Physics Review 57, 5726–5792.

Farrand, W.H., Singer, R.B., 1992. Alteration of Hydrovolcanic Basaltic Ash: Observations with visible and near-infrared spectrometry. Journal of Geophysical Research 97 (B12), 393–408.

Fisher, R.V., 1961. Proposed classification of volcaniclastic sediments and rocks. Geological Society of America Bulletin 72, 1409–1414.

Fisher, R.V., Schmincke, H.U., 1984. Pyroclastic Rocks. Springer-Verlag, Berlin, Federal Republic of Germany (DEU).

Godchaux, M.M., Bonnichsen, B., 2002. Syneruptive magma-water and posteruptive lava-water interactions in the western Snake River Plain, Idaho, during the past 12 million years. In: Bonnichsen, B., White, C.M., McCurry, M. (Eds.), Tectonic and

Magmatic Evolution of the Snake River Plain Volcanic Province. Idaho Geological Survey Bulletin, vol. 30, pp. 387–434.

Godchaux, M.M., Bonnichsen, B., Jenks, M.D., 1992. Types of phreatomagmatic volcanoes in the western Snake River Plain, Idaho, USA. Journal of Volcanology and Geothermal Research 52, 1–25.

Heiken, G.H., 1971. Tuff rings: examples from the Fort Rock-Christmas Lake Valley basin, south-central Oregon. Journal of Geophysical Research 76, 5615–5626.

Heiken, G.H., Wohletz, K.H., 1986. Volcanic Ash. University of California Press, Berkeley.

Houghton, B.F., Wilson, C.J.N., 1989. A vesicularity index for pyroclastic deposits. Bulletin of Volcanology 51, 451–462.

Kokelaar, B.P., 1983. The mechanism of Surtseyan volcanism. Journal of Geological Society of London 140, 939–944.

Lorenz, V., 1986. On the growth of maars and diatremes and its relevance to the formation of tuff rings. Bulletin of Volcanology 48 (5), 265–274.

Mabey, D.R., 1982. Geophysics and tectonics of the Snake River Plain, Idaho. In: Bonnichsen, B., Breckenridge, R.M. (Eds.), Cenozoic Geology of Idaho. Idaho Geological Survey Bulletin, vol. 26, pp. 139–154.

Malde, H.E., 1987. The Montini volcano; A lava dam on the ancestral Snake River, southwest Idaho. Geological Society of America Centennial Field Guide Volume 2. Rocky Mountain Section, pp. 127–130.

Malde, H.E., Powers, H.A., 1962. Upper Cenozoic stratigraphy of the western Snake River Plain, Idaho. Geological Society of America Bulletin 73, 1197–1220.

Moore, J.G., 1985. Structure and eruptive mechanisms at Surtsey volcano, Iceland. Geological Magazine 122, 649–661.

Morrissey, M., Zimanowski, B., Wohletz, K., Buettner, R., 2000. Phreatomagmatic fragmentation. In: Sigurdsson, H., Houghton, B., McNutt, S.R., Rymer, H., Stix, J. (Eds.), Encyclopedia of Volcanoes. Academic Press, London, pp. 431–445.

Németh, K., Martin, U., Harangi, Sz., 2001. Miocene phreatomagmatic volcanism at Tihany (Pannonian Basin, Hungary). Journal of Volcanology and Geothermal Research 111, 111–135.

O'Conner, J.E., 1993. Hydrology, hydraulics, and geomorphology of the Bonneville flood. Geological Society of America Special Paper 274, 83.

Othberg, K.L., 1994. Geology and geomorphology of the Boise Valley and adjoining areas, western Snake River Plain, Idaho. Idaho Geological Survey Bulletin 29, 54.

Pierce, K.L., Morgan, L.A., 1992. The track of the Yellowstone hotspot: Volcanism, faulting, and uplift. In: Link, P.K., Kuntz, M.A., Platt, L.B. (Eds.), Regional Geology of Eastern Idaho and Western Wyoming. Geological Society of America Memoir, vol. 179, pp. 1–53.

Rosi, M., 1992. A model for the formation of vesiculated tuff by the coalescence of accretionary lapilli. Bulletin of Volcanology 54, 429–434.

Schmid, R., 1981. Descriptive nomenclature and classification of pyroclastic deposits and fragments: recommendations of the IUGS subcommission on the systematics of igneous rocks. Geology [Boulder] 9, 41–43.

Sheridan, M.F., Wohletz, K.H., 1983. Hydrovolcanism: Basic considerations and review. Journal of Volcanology and Geothermal Research 17, 1–29.

Sohn, Y.K., Chough, S.K., 1989. Depositional processes of the Suwolbong tuff ring, Cheju Island (Korea). Sedimentology 36, 837–855.

Waters, A.D., Fisher, R.V., 1971. Base surges and their deposits: Capelinhos and Taal volcanoes. Journal of Geophysical Research 76, 5596–5614.

White, J.D.L., 1996. Pre-emergent construction of a lacustrine basaltic volcano, Pahvant Butte, Utah (USA). Bulletin of Volcanology 58, 249–262.

White, J.D.L., 2001. Eruption and reshaping of Pahvant Butte Volcano in Pleistocene Lake Bonneville. Special Publication of the International Association of Sedimentologist 30, 61–80.

White, J.D.L., Houghton, B., 2000. Surtseyan and related phreatomagmatic eruptions. In: Sigurdsson, H., Houghton, B., McNutt, S.R., Rymer, H., Stix, J. (Eds.), Encyclopedia of Volcanoes. Academic Press, London, pp. 495–511.

Wohletz, K.H., 1986. Explosive magma-water interactions: thermodynamics, explosion mechanisms, and field studies. Bulletin of Volcanology 48, 245–264.

Wohletz, K.H., McQueen, R.G., 1984. Experimental Studies of Hydromagmatic Volcanism. Studies of Geophysics. National Academic Press, Washington, pp. 158–169.

Wohletz, K., Sheridan, M.F., 1979. Model of Pyroclastic Surge. Geological Society of America Paper 180.

Wood, S.H., Clemens, D.M., 2002. Geologic and tectonic history of the western Snake River Plain, Idaho and Oregon. In: Bonnichsen, B., White, C.M., McCurry, M. (Eds.), Tectonic and Magmatic Evolution of the Snake River Plain Volcanic Province. Idaho Geological Survey Bulletin, vol. 30, pp. 387–434.